

Hydrogen-Bond-Induced Microstructural Transition of Ionic Micelles in the Presence of Neutral Naphthols: pH Dependent Morphology and Location of Surface Activity

Moazzam Ali, Mrinmoy Jha, Susanta K. Das, and Swapan K. Saha*

Department of Chemistry, University of North Bengal, Darjeeling 734 013, India

Received: August 9, 2009

The effect of naphthols and methoxynaphthalenes on the microstructure transition of cetyltrimethylammonium bromide (CTAB) micelles is studied. Although the surface activities of these two types of organic dopants are strong, methoxynaphthalenes failed to promote spherical to worm-like micellar transition and to impart viscoelasticity to the aqueous CTAB solution, presumably due to their inability to form unique H-bonds with interfacial water. The micropolarity of OH sites of micelle-embedded naphthols is measured by observing the pK_a shift at the micellar surface relative to bulk water. On the basis of spectroscopic and other data, the microstructures formed by both classes of dopants at the micellar surface are predicted. On the basis of hydroxyaromatic dopants, a simple and effective route to design pH-responsive viscoelastic worm-like micelles and the vesicles of single tail cationic surfactant (CTAB) is reported. Results are confirmed by observing cryogenic transmission electron microscopy (cryo-TEM) images.

Introduction

Organic π -conjugated molecules are effective tuners in the formation of various nanostructured materials, and the entailed route is potentially facile and efficient for the development of functional materials of technological and biological importance.^{1–4} Microstructural transitions of micellar aggregates, especially the nature of transition from ordinary micelles to long worm-like giant micelles and the vesicles, mediated by organic π -electron systems are of fundamental scientific interest and have been reported in several papers recently.^{5–8} Moreover, synthetic vesicular systems are interesting from a number of standpoints, not the least being their structural similarity with the constituent of the biomembrane, viz., phospholipid. They offer a convenient way to probe interactions involving membrane systems. Vesicle aggregation or adhesion is the primary step for the fusion of the vesicles in membrane. Therefore, the elucidation of the molecular mechanism of vesicular aggregation would greatly contribute to a better understanding of these biological phenomena. Single chain ionic surfactants, e.g., cetyltrimethylammonium bromide (CTAB), favor convex-up surface geometry of the micelles due to strong headgroup repulsion and form spherical or near spherical micelles at the critical micelle concentration (cmc), while either at much higher surfactant concentrations (~ 1.0 M) or in the presence of high inorganic salt concentrations (>0.1 M), morphological changes occur to rod-like micelles and vesicles.^{9–12} Hydrotropic salts like sodium salicylate (SS) also promote sphere to worm-like micellar transition at considerably lower concentration (e.g., ~ 1.0 mM in CTAB) by increasing the packing parameter above the critical value of 1/3 via efficient charge screening of the surfactant head groups.¹³ These worm-like micellar solutions at low concentrations show complex and unusual rheological phenomena. They exhibit some fascinating shear dependent properties and have been the subject of much discussion for a long time.^{14–18} For example, when sheared below a critical shear rate which depends on temperature, surfactant, and salt concentrations, dilute worm-

like micellar solutions shear thin. On the contrary, above a critical shear rate, micellar solutions show time dependent behavior. Initially, the solutions shear thin, and after an induction period, the solutions exhibit a shear thickening property. It has been suggested that shear thickening occurs because free worm-like micelles join a transient network under shear; the microstructures have been broadly named shear-induced structure or phase (SIS or SIP, respectively).^{19–21} However, in certain systems, e.g., cetyltrimethylammonium chloride/sodium 3-methyl salicylate dispersion, vesicle to worm-like micellar transition and vice versa have been claimed to occur under shear, leading to rheological modification of the system.²² A recent discovery of the flow-induced structure transition between vesicle and micelle is also interesting. The structural transition induced by flow in the cetyltrimethylammonium 3-hydroxy naphthalene 2-carboxylate micelles and the mixture of hexadecylpyridinium chloride and sodium chlorate caused initial confusion because there has been apparently no reason for how the structural transition takes place.^{22,23} As has already been pointed out, a facile and interesting route of lowering the surface curvature of micelles of single chain cationic surfactants is to increase the effective cross-sectional area of the hydrocarbon tail and to shield the headgroup charges by embedding neutral aromatic compounds with hydrogen bonding functionalities (e.g., 1- and 2-naphthols).⁵ These dopants upon embedding in the micelle hinder any curvilinear displacement of head groups to take place via a comparatively rigid network of hydrogen bonding at the micelle surface and at the same time decrease the area of the surfactant head groups efficiently. The efficiency of hydroxy aromatic compounds in micellar shape transition is very high, and an aqueous mixture of CTAB and 2,3-dihydroxy naphthalene which gives highly viscous rod-like nanoaggregates has been used as a template for the sol–gel synthesis, providing an aqueous route for tube silicate preparation.⁷ Altering the structure of the micellar system by phenolic dopant is an easy way to tailor the structure and properties of mesoporous materials which are synthesized on the micellar templates.²⁴ UV absorption spectra are modified due to the presence of an intermolecular H-bond in micelle-embedded naphthols in their ground elec-

* To whom correspondence should be addressed. E-mail: ssahanbu@hotmail.com.

tronic states, and this was confirmed by FTIR. The excited state proton transfer (ESPT) of 2-naphthol is facilitated in the presence of CTAB in the submicellar concentration range due to the catalytic effect of surfactant charge, whereas ESPT is hindered in post-micellar concentrations due to lack of water accessibility. However, the exact nature of H-bonding in the micellar phase is not understood completely. Moreover, together with hydrogen bonding, the π - π and cation- π interactions between favorably arranged micelle-embedded naphthol molecules may also be involved in modifying the absorption spectra.²⁵ Therefore, in order to further examine the exact nature of the noncovalent interaction that is involved in the above modification of the spectra, it is tempting to check what would happen if we replace the hydroxyl group of the promoter naphthol molecules by methoxy groups. Methoxy naphthalenes (MN) possess a similar structure and hydrophobicity to that of the naphthol (HN) molecules but cannot act as hydrogen bond donors. It would be interesting to compare the efficiency of methoxy naphthalenes with that of naphthols in effecting microstructural transitions of micelles and to discuss the result in the light spectroscopic observations. Further, it may be anticipated that a simple and effective route to design a pH-responsive microstructure could well be based on the neutral naphthol dopants, which form salts only at high pH ($pK_a > 9.2$). As a function of pH, ionization of the OH group of naphthol molecules may switch the onset of charge screening, paving the way to effect further morphological transitions (viz., vesicle formation). An objective of the present work is, therefore, to design a simple effective route of pH-responsive morphological transition for the aqueous molecular aggregates of single chain cationic surfactant, viz., CTAB from micelles to long worm-like micelle to unilamellar vesicles.

Finally, it is important to note that although the last two decades have witnessed a strong excitement among the researchers on the microstructural transitions of micelles at low concentrations, induced by hydrotropes like sodium salicylate and other similar dopants, leading to stimuli-responsive viscoelasticity, the exact role and the location of the protruded polar groups (e.g., OH groups) of the hydrotropes toward the Stern layer have not been firmly ascertained. This is particularly an interesting basic element to investigate for the present system where intermolecular H-bonding through OH groups of the micelle-embedded naphthols seems to play the pivotal role in the transition of the micellar morphology. In this work, therefore, micropolarity has been determined at the OH group sites by monitoring the pK_a shift at the micellar interface relative to bulk water in an attempt to determine the location of the protruded OH groups in the Stern layer.^{26,27}

Experimental Section

1- and 2-Naphthols (puriss, Aldrich) were purified by vacuum sublimation followed by crystallization from 1:1 aqueous methanol. 1- and 2-Methoxynaphthalenes (Acros-Organics, Belgium) were recrystallized from 1:1 aqueous methanol before use. CTAB (puriss, Aldrich) was used as received. ¹H NMR and UV absorption spectra were recorded on a Bruker (300 MHz) spectrometer and a Jasco (v-530) spectrophotometer, respectively. Shear-induced viscosity was measured on a rotational viscometer (Anton-Paar, DV-3P; accuracy $\pm 1\%$ and repeatability $\pm 0.2\%$) equipped with a temperature controller and with the facility of varying shear rates. A Kruss tensiometer (K 9) was used for surface tension measurements. Sample preparation on a TEM grid for cryo-TEM study was done following a similar method to that described in a previous paper.⁵

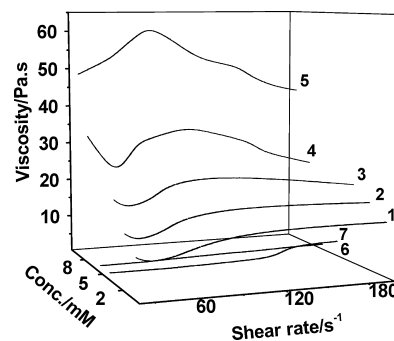


Figure 1. Steady shear viscosity as a function of the applied shear rate for dilute and concentrated solutions of 2-naphthol/CTAB at 25 °C. The molar concentration ratio, [2-naphthol]/[CTAB], was fixed at unity. (1) 1.0, (2) 1.5, (3) 2.0, (4) 5.0, (5) 8.5 mM. (6) and (7) are plots for 1- and 2-methoxynaphthalene-CTAB (5 mM, 1:1) systems, respectively.

Results and Discussion

Shear-Induced Viscoelasticity and Surface Activity: Role of the OH Group of the Dopant. Figure 1 shows the rheological responses for a representative viscoelastic system, viz., an aqueous CTAB-1-naphthol system as a function of concentration (1:1 mol ratio; this composition yields the strongest viscoelasticity) at 25 °C (pH ~ 5.0). At low concentrations (< 2 mM), this system shows a shear thinning property up to a shear rate of 25 s^{-1} and then the shear thickening phenomenon starts to occur, but above a shear rate of 60 s^{-1} , the fluid shows a Newtonian type behavior (Figure 1(1,2)). However, an overall non-Newtonian nature is apparent as the concentration of the CTAB and naphthol (1:1) system is raised above 2.0 mM. At still higher concentrations (> 5.0 mM), the nature of the rheological response changes dramatically and the system starts displaying an unusual rheology as a function of shear rate (Figure 1(4)). Up to a shear rate of 60 s^{-1} , the fluid shear thins. An onset of viscosity rise is observed at the shear rate of 60 s^{-1} , and the system again shear thins, passing through a maximum at 70 s^{-1} . At further higher concentrations (8.5 mM), the viscosity-shear rate profile again changes feature; the initial shear thinning characteristics disappear. The overall behavior is consistent with building up of long worm-like micellar bundles at relatively high concentrations. Therefore, it appears that the shear thinning viscosity in low shear rates is indicative of the flow-induced alignment toward the flow directions. Meanwhile, when the CTAB concentration is above 10.0 mM in the equimolar CTAB/naphthol solutions, the micelles are much longer and entangled with each other in the solution. In this case, the shear viscosity increases much higher and the micellar solution behaves like entangled polymer solutions exhibiting typical nonlinear viscoelastic behavior such as a stress plateau. The contour length of the worm-like micelles is highly dependent on the concentrations of the surfactant and the promoter.

The methoxynaphthalene-CTAB systems, on the other hand, neither display the ability to develop viscoelasticity (6,7 of Figure 1) in the system nor exhibit any viscosity modification with applied shear, and behave completely like a Newtonian liquid. This result is quite surprising in view of the fact that much like 1- and 2-naphthols, both 1- and 2-methoxynaphthalene are expected to embed into the micelles of CTAB. Therefore, to ascertain the location and orientation of the additive methoxy naphthalene molecules in the micelles and to understand the nature of the interaction with micelles, ¹H NMR experiments were performed (Figure 2).

The NMR spectrum of 1-MN in D₂O (in the absence of CTAB) shows four sets of signals, centered at δ values of 8.151,

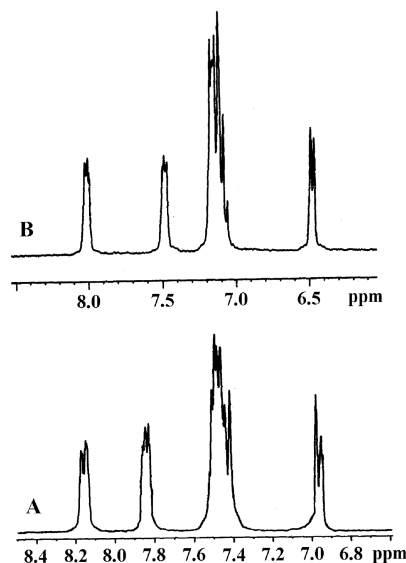


Figure 2. ^1H NMR spectra of 1-methoxynaphthalene in the absence (A) and presence (B) of CTAB (7.5 mM, 1:1).

7.853, 7.482, and 6.947, respectively, due to the resonance of the aromatic ring protons (Figure 2A). All four sets of signals are shifted upfield, remain well resolved, and appear at δ values of 8.013, 7.492, 7.147, and 6.487, respectively, when D_2O solutions of CTAB and 1-MN are mixed in 1:1 molar ratio (7.5 mM; Figure 2B). The methoxy protons which resonate at a δ value of 3.953 in water (not shown) are also shifted upfield and resonate at a δ value of 3.561 in CTAB. A similar upfield shift of aromatic and methoxy proton signals is observed in the CTAB–2-MN system as well. This large shift of either aromatic proton resonance or methoxy proton resonance to low δ values clearly indicates the location of naphthalene rings as well as the methoxy group of methoxy naphthalene molecules in the less polar environment than that of water. A previous study with the CTAB–naphthol system also showed a similar upfield shift of proton resonance of the aromatic moiety of the naphthol molecule, and it was argued that this was due to insertion of naphthol molecules into the micelle.⁵ Unlike naphthol–CTAB systems, absence of line broadening and the well resolved structures of the NMR signals clearly indicates fast rotation of naphthalene rings in the CTAB–MN systems (on the NMR time scale). However, the degree of upfield shift of the signals is less in 1-MN than that in naphthols; this indicates a stronger

partitioning of naphthol molecules in the micelles. In this context, comparison of surface activities of methoxynaphthalenes and naphthols may also be interesting.

Figure 3 clearly shows that both 1- and 2-naphthols reduce the surface tension (ST) of water to a considerable extent, indicating that naphthols are surface active. Previously, it has been shown that 3-hydroxynaphthalene 2-carboxylate (SHNC) also reduces the surface tension in a similar manner and it also effectively promotes micellar shape transition.²⁸ Interestingly, while SHNC decreased the surface tension of water from a value of 75 to 60 N/m in the presence of 60 mM concentration of SHNC, an identical decrease in surface tension has been brought about by naphthols in the presence of only 0.4 and 0.5 mM concentrations. On the other hand, the surface tension of water is decreased to a similar extent by an even lesser amount of 1- and 2-MN's. While 1-MN decreases the ST of water up to the extent of 58 mN in the presence of 0.31 mM concentration, 2-MN did the identical ST lowering in the presence of only 0.16 mM concentration. While the extents of surface activity displayed by both naphthols are very close to each other, for 1- and 2-MN molecules, it differs quite significantly (Figure 3). The result indicates that 1- and 2-methoxy naphthalenes are stronger surface active agents than 1- and 2-naphthols, and accordingly, these molecules are expected to be embedded into the micelle strongly. Therefore, the findings of the NMR experiment are further strengthened by this fresh evidence of surface activities exhibited by methoxy naphthalene molecules. However, in spite of the strong surface activity shown by 1- and 2-MN, they fail to induce a microstructural transition in CTAB micelles. It seems apparent that OH groups in naphthol molecules play an important role in this respect. The results show that the naphthols are involved in a stronger and different kind of interaction with CTAB micelles as compared to methoxy naphthalenes. The surfactant, viz., CTAB, forms spherical micelles in the presence of methoxynaphthalene (2–10 mM; 1:1), whereas in the presence of naphthols CTAB forms long worm-like micelles and even vesicles (discussed in a later part).

Microscopic Polarity at the Location of OH Groups of Embedded Naphthols. It is believed that while the aromatic rings of naphthols are embedded in micelles, the core of which having a dielectric constant around 2–7 only, the OH groups stand out toward the water region. NMR study also confirms that the aromatic ring of the naphthol resides near the nonpolar core in between tetraalkylammonium head groups of the surfactants. Although almost all of the previous studies on the

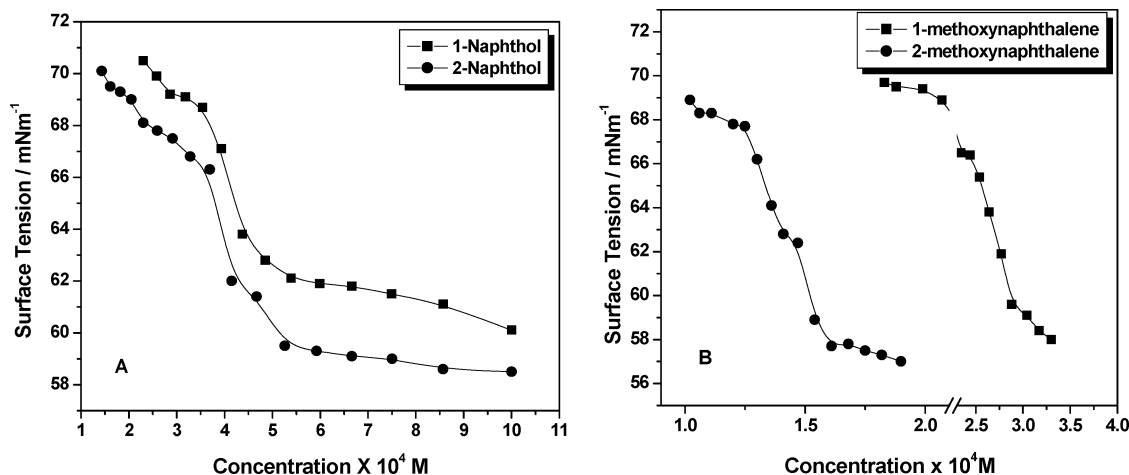
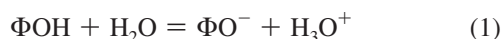


Figure 3. Surface tension of naphthols (A) and methoxynaphthalenes (B) as a function of concentration in water at 25 °C.

hydrotrope-induced microstructural transitions of micelles argue that the OH groups protrude out of the micellar surface and remain close to the aqueous layer, no experimental verification has so far been reported. To understand the exact nature of the location of the OH group, the micropolarity of the residence sites is determined. Spectral characteristics, especially fluorescence spectra, are often very sensitive to the environments around the probe molecule. Because of this, fluorescence spectroscopy has become one of the important methods for the study of the structure and dynamics of the microheterogeneous systems. Unfortunately, the excited state proton transfer process (ESPT) of hydroxyaromatic compounds, viz., 1- and 2-naphthols, complicates their spectral properties. The absorption spectra are also not sensitive to the environmental conditions in the present system. Moreover, information regarding the microenvironment of the aromatic π -electron system, which might have been obtained from the study of spectral characteristics, would not be helpful in determining the location of protruded OH groups of naphthol molecules. Therefore, pK_a shift of the acid–base equilibrium of the OH group of naphthols in a microheterogeneous medium relative to aqueous solution would be the ideal route for getting such information precisely. This shift in pK_a in a cationic micelle like CTAB relative to aqueous solution may be due to the surface potential of the micelle and the polarity variation at the micellar interface from that of the bulk (in the absence of any specific interaction). The theoretical background of the analysis of data pertaining to the interfacial acid–base equilibrium of naphthol molecules has been well documented for other similar probes.^{26,27} While determining pK_a values of the present system, let us assume that the acid–base equilibrium of the OH group of naphthols is described by



where ΦO^- , ΦOH , and H_3O^+ are deprotonated and protonated (neutral) forms of the naphthols and the proton, respectively. For the naphthol indicators in aqueous micellar solution, the apparent pK_a values were obtained from the change in the ultraviolet absorption spectra as a function of bulk aqueous pH by means of the following Henderson–Hasselbach equation (which considers only concentration terms at low concentration conditions) as follows (eq 1):

$$pK_a^{obs} = pH - \log[\Phi O^-]/[\Phi OH] \quad (1a)$$

provided that the quantity $[\Phi O^-]/[\Phi OH]$ is determined by $(A - A_{\Phi OH})/(A_{\Phi O^-} - A)$, where A , $A_{\Phi OH}$, and $A_{\Phi O^-}$ are the absorbances of naphthols at experimental pH and low and high pH's, respectively. The near UV spectra of 1-naphthol as a function of the bulk aqueous pH in CTAB micelle solution are shown in Figure 4 (unfortunately, the spectral profile of 2-naphthol is insensitive toward bulk aqueous pH and, therefore, cannot be studied). For the acid–base equilibrium of the interfacially located organic molecule, the pK_a^{obs} is now separated into two components, viz., an electrostatic component and a nonelectrostatic environmental component. This is formalized in relation 2

$$pK_a^{obs} = pK_a^0 - e\Psi_0/2.303kT \quad (2)$$

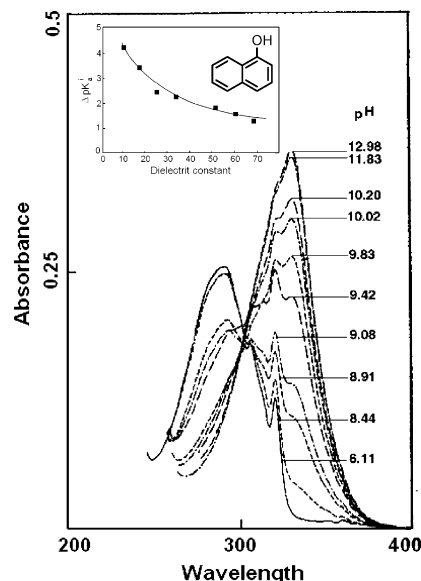


Figure 4. UV absorption spectra of 1-naphthol (0.5 mM) in 5.0 mM CTAB at varying pH.

where pK_a^0 is the apparent pK_a value if the surface potential of the micelle, Ψ_0 , is null. Information can be obtained about the acid–base equilibrium at the surfactant–water interfaces by comparing pK_a^0 values of naphthols in the aqueous micellar systems with the pK_a values for naphthols in the aqueous–organic mixtures, e.g., dioxane–water mixtures. The apparent pK_a in organic–aqueous mixture, pK_a^m , is defined in the following relation (eq 3).

$$pK_a^m = B + \log U_H^0 - \log[\Phi O^-]/[\Phi OH] - \log \gamma_{\Phi O^-}^m / \gamma_{\Phi OH}^m \quad (3)$$

where γ^m 's are activity coefficient terms in the medium, B is the pH meter reading, and $\log U_H^0$ is the correction factor to be applied to pH meter reading to measure the actual hydrogen ion concentration in organic–aqueous mixtures. The pK_a^0 values relate to a system where the conjugate acid–base species reside in an interfacial microenvironment but the bulk aqueous solution pH is measured. Hence, the comparison between pK_a values in dioxane–water mixtures and pK_a^0 values in micelle systems should take into account the primary medium effect on the proton. In other words, pK_a^0 values need to compare to pK_a^i values rather than pK_a^m 's where

$$pK_a^i = pK_a^m + m\gamma_H^+ \quad (4)$$

and $m\gamma_H^+$ denotes the primary medium effect on the proton. It is usual to assume that the mean primary medium effect on HCl, $m\gamma_{\pm}$, approximates to $m\gamma_H^+$. The $\log U_H^0$ and $m\gamma_{\pm}$ values given in refs 26 and 27 were employed to derive pK_a^i values in dioxane–water mixtures. These pK_a^i ($\Delta pK_a^i = pK_a^i - pK_a^w$) values as a function of medium dielectric constant are shown in Figure 4 (inset). The pK_a^0 values of 1-naphthol in CTAB micelles are determined with the aid of eq 2 and the known value of the surface potential of CTAB micelles of +141 mV.²⁶ The effective dielectric constant (D_{eff}) values are obtained by comparing ΔpK_a^0 's (Table 1) of 1-naphthol on a micellar surface with ΔpK_a^i values in 1,4-dioxane–water mixtures (Figure 4; inset). It may be noted that D_{eff} values

TABLE 1: Results of pH Titration of 1-Naphthol in Aqueous and Aqueous CTAB Micellar Solution at 25°C

conc. of CTAB/mM (conc. of 1-HN = 0.5 mM)	pK_a^w	pK_a^{obs}	$-\Delta pK_a^{obs}$	pK_a^0	ΔpK_a^0
20		8.623	0.765	11.007	1.619
50	9.388	8.679	0.709	11.063	1.675
100		8.914	0.474	11.298	1.910

TABLE 2: D_{eff} Values of OH Group Location of Micellar Interface

conc. of CTAB/mM (conc. of 1-HN = 0.5 mM)	D_{eff}
20	51 ± 3
50	49 ± 3
100	45 ± 2

are measured on the basis of several assumptions: (i) both the protonated and deprotonated forms of the naphthol indicator are quantitatively partitioned into the micellar phase at least at high surfactant/naphthol ratio; (ii) the activity coefficient term ($\log \gamma_{\text{FO}}^i / \gamma_{\text{FOH}}^i$) is negligibly small so that ΔpK_a^0 values are directly comparable with the ΔpK_a^i behavior in different solvent dielectric constant bulk media; (iii) although the OH groups of naphthol protrude from the micellar surface, the acid–base equilibrium is still under the influence of micellar surface potential; (iv) it is evident that much like the 1,4-dioxane–naphthol system, the interfacial water of CTAB micelles forms H-bonds with micelle-embedded naphthols (discussed later), which act as a H-donor in both of the above cases. No serious error in the evaluation of D_{eff} due to the presence of this H-bond is thus anticipated because such an effect, if any, would be compensated by the similar interaction present in the reference system (naphthols in dioxane–water).

Table 2 shows that D_{eff} at the interface of CTAB micelles, as measured by the pK_a shift of interfacially located naphthols, varies from 51 ± 3 to 45 ± 2 as a function of CTAB concentration from 20 to 100 mM (concentration of naphthol being 0.5 mM throughout). This result indicates that naphthols are increasingly partitioned in micelles as the CTAB concentration is increased. Utilizing the solvatochromic visible absorption band maximum $E_T(30)$, D_{eff} estimates of 28–33 were obtained previously for CTAB micelles.²⁹ Therefore, in comparison to the previously determined micropolarity of the CTAB micellar surface ($D_{eff} \sim 30$), the present value of 45 (under conditions when most of the naphthol molecules are partitioned in micelles) is substantially high. This is an interesting observation. This clearly indicates that the OH groups are directed away from the surface of the micelles and are located around the more polar region. Assuming a polarity gradient to exist with the distance from the micellar surface, one can have a rough idea of the location of the OH groups in the Stern layer. A recent application of numerical Poisson–Boltzmann methods to the determination of the electrostatic potential and counterion distribution around polyelectrolyte such as DNA may be relevant in this respect.³⁰ In this case, the situation had prompted us to choose a dielectric constant “field”, where low dielectric values exist near 30 at the polyelectrolyte surface and increase away to the values near 78.5 in bulk water. A rough estimation following the above work, which takes on a cylindrical polyelectrolyte (e.g., DNA) surface of radius 10 Å as the low dielectric region, shows that the present D_{eff} value of 45 (compared to ~ 30 at the micellar surface) could be rationalized assuming the OH group of naphthol to be protruded away

from the CTAB micellar surface through a nearly 1 Å distance toward the Stern layer.³⁰

Spectral Modification of Micelle-Embedded Dopants: Contribution of H-Bonding, π – π or Cation– π Interactions?

In view of the differences in the viscoelastic responses and the morphological transitions of CTAB micelles (Figure 1) induced by neutral naphthols and the methoxy naphthalenes, UV absorption spectra of these dopants may be interesting to study in micellar media. To understand the kind of interactions which are operative in the micelle–dopant systems, the key element of the present study is to compare the spectral characteristics of naphthols (HNs which contain OH) with those of methoxy naphthalenes (MNs, which do not contain OH) under various conditions in order to visualize a consistent molecular picture eliminating the untenable suggestions. Aromatic compounds, e.g., naphthalene, in general, have two strongly overlapped bands in the near UV region, viz., the longitudinally polarized $^1L_a \leftarrow ^1A$ band and the transversely polarized $^1L_b \leftarrow ^1A$ band. While the vibrational structure of these bands appears differently in different substituted compounds, effects of extending conjugation in 1 and 2 positions by OH or CH₃O groups in naphthol and methoxynaphthalene molecules, respectively, are interesting. Both in 1-naphthol and 1-methoxy, naphthalene conjugation is extended in the transverse direction and, therefore, it affects the transverse polarized 1L_a band. In 2-naphthol and 2-methoxy naphthalene, on the other hand, conjugation is primarily extended in the longitudinal direction, affecting both the intensity and the frequency of the longitudinally polarized 1L_b band compared to the unsubstituted naphthalene.

It is well-known that the near UV spectra of aromatic compounds are affected by specific interactions like hydrogen bonding. Noncovalent interactions like π – π and cation– π also cause shifts in the electron distributions of the molecule. The OH group of naphthols can act as both a proton donor as well as a proton acceptor in forming intermolecular hydrogen bonding. A hydrogen bond in which the hydroxyl groups of naphthols is a proton donor releases electron density from the O–H bond toward the oxygen and hence, by an inductive effect, toward the aromatic ring. This causes a red-shift of the π – π^* transition. Conversely, if a hydrogen bond is formed in which the hydroxyl oxygen is a proton acceptor, electrons are withdrawn from the naphthalene ring, and an opposite shift is anticipated. If both bonds could form at the same time and with equal ease, since their effects on the partial charges of the oxygen are opposite, the net change on the oxygen and hence on the aromatic ring may be small. Therefore, in such a situation, the spectral shift relative to the position of the band in a non-hydrogen-bonding situation ought to be small.³² The near UV absorption of 1-naphthol which arises from two strongly overlapped π – π^* transitions remains unaffected in the presence of submicellar aqueous CTAB solution, indicating the absence of any appreciable interaction (Figure 5) (the effect of CTAB micelles on the UV spectra of 2-naphthol is also similar). However, interestingly, significant red-shift starts to occur (6.4 nm at $\lambda_{\text{max}} \sim 293$ nm) in the presence of CTAB just above its cmc (0.96 mM) with a well-defined isobastic point at 296 nm. Such shifting of λ_{max} continues until most of the naphthol molecules are partitioned in the micellar phase at high surfactant/naphthol ratio (80:1; Figure 5A). The result suggests that the protruded OH groups of micelle-embedded naphthols form a H-bond with interfacially located ($D_{eff} \sim 45$) water molecules and act as a H-donor. It may also be argued that at a mole ratio of 1:1 of naphthol and the CTAB, at which maximum viscoelastic response is observed under shear due to the presence

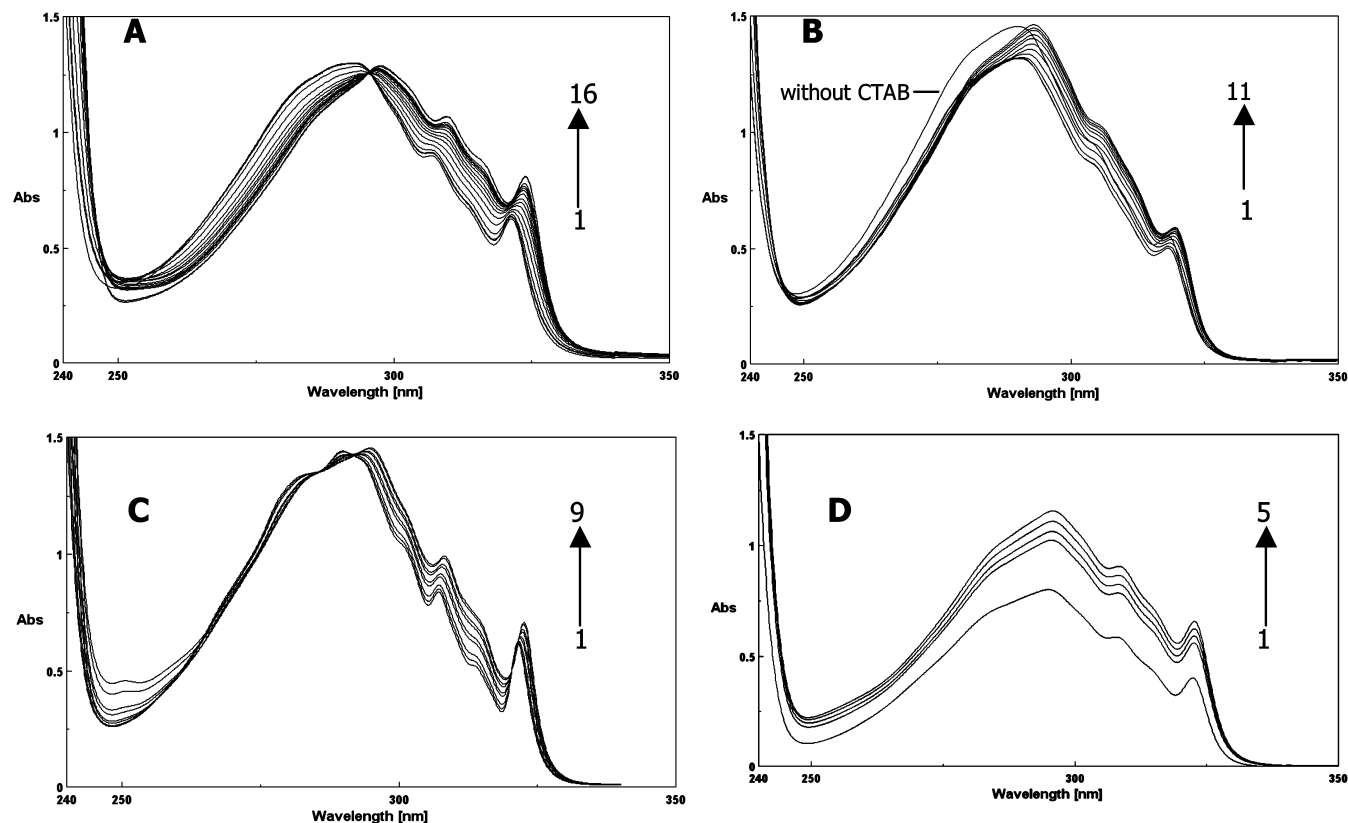


Figure 5. (A) Absorption spectra of 1-HN (0.25 mM) in water at varying concentrations of CTAB at 25 °C. [CTAB]: (1) 0.0, (2) 0.44, (3) 0.55, (4) 0.75, (5) 1.00, (6) 1.25, (7) 1.50, (8) 1.75, (9) 2.00, (10) 2.50, (11) 3.00, (12) 3.50, (13) 4.00, (14) 5.00, (15) 15.00, (16) 20.00 mM. (B) Absorption spectra of 1-HN (0.25 mM) in water at varying concentrations of CTAB at 25 °C. [CTAB]: (1) 0.33, (2) 0.50, (3) 0.75, (4) 1.00, (5) 1.50, (6) 2.00, (7) 2.50, (8) 3.00, (9) 3.50, (10) 4.00, (11) 5.00 mM. (C) Absorption spectra of 1-HN (0.25 mM) in isooctane at various concentrations of 1,4-dioxane at 25 °C. [Dioxane]: (1) 0.00, (2) 13, (3) 20, (4) 40, (5) 50, (6) 80, (7) 100, (8) 160, (9) 200 mM. (D) Absorption spectra of 1-HN (0.25 mM) in acetonitrile at different percentages of water at 25 °C. % of water: (1) 0.00%, (2) 4%, (3) 6%, (4) 8%, (5) 10%.

of entangled worm-like micelles, not all of the naphthol molecules are embedded in the micelles, but some are located in the palisade layer. These naphthols may, however, be involved in H-bond network formation with embedded molecules via interfacial water.

The spectral feature (Figure 5A) and the nature and degree of shift undoubtedly resemble the spectra of naphthol in isooctane at various dioxane concentrations (red-shift of 6.3 nm at $\lambda_{\text{max}} \sim 293$ nm, Figure 5C, as compared to a red-shift of 6.4 nm at $\lambda_{\text{max}} \sim 293$ nm, Figure 5A) where naphthol acts as the hydrogen bond donor and dioxane as the acceptor (Figure 5C).³¹

Previously, it has been shown that, in the ground state, 1-naphthol interacts with water via oxygen, whereas with alcohols (ethanol and isopropanol) and acetonitrile it interacts via hydrogen from the hydroxyl group.³³ The nature of spectral modification encountered by micelle free naphthol molecules in the presence of water is shown in Figure 5D. This figure shows that on every addition of water (up to 10% v/v) substantial gain in intensity is displayed by 1-naphthol spectra (in acetonitrile) with little change of wavelength. The nature of spectral modification of 1-HN due to H-bond formation is quite different from that of micelle-embedded naphthol. It may be argued that, like alcohols and acetonitrile media, naphthols at the interface ($D_{\text{eff}} \sim 45$) act as H-donating agents and water as a H-acceptor at the oxygen atom. This is indeed interesting. The low D_{eff} value found for the interfacial microenvironment of CTAB micelles may be attributed to a low interfacial water activity. Nevertheless, it has also been argued that the low interfacial D_{eff} value may be a result of the H-bond donor properties of

the water in the interfacial region being different from that of bulk water, and/or the presence of electrostatic image interactions caused by the proximity of the low dielectric hydrocarbon core. Present experiments indeed justify the former conjecture precisely.³⁴ It is known that the water molecules at the micellar interface have some strange properties.^{35,36} The solvation dynamics are slowed down by several orders of magnitude relative to bulk water. The reorientational motion is also restricted. The dynamics of water molecules near an aqueous micellar interface has been a subject of intense current interest because such a system serves as a prototype of complex biological system. Furthermore, oxygen K absorption and emission spectra of water molecules in the micellar interface also show that the local electronic structure of water molecules is dramatically different from that of bulk water.³⁷ The relatively less polar and less mobile water molecules compared to bulk water form a strong H-bond with the OH group of embedded naphthols, which act as H-donors and result in an optimum orientation of aromatic π -electron systems in the micelles to shield the surfactant headgroup charges efficiently; maybe via cation- π interaction; i.e., the cation charge of surfactant head groups interacts with the quadrupole moment of the aromatic π -system of naphthols. On the other hand, as the H atom of OH is replaced by a CH_3 group (viz., the methoxy naphthalene molecule), the ability of intermolecular H-bond formation disappears. Instead, the H-accepting tendency from a potential donor is enhanced. The nature of changes encountered in the UV spectra of methoxy naphthalenes on the addition of CTAB above its cmc indicates the permeation of the dopant molecules in the micelles (Figure 5B). The small red-shift compared to

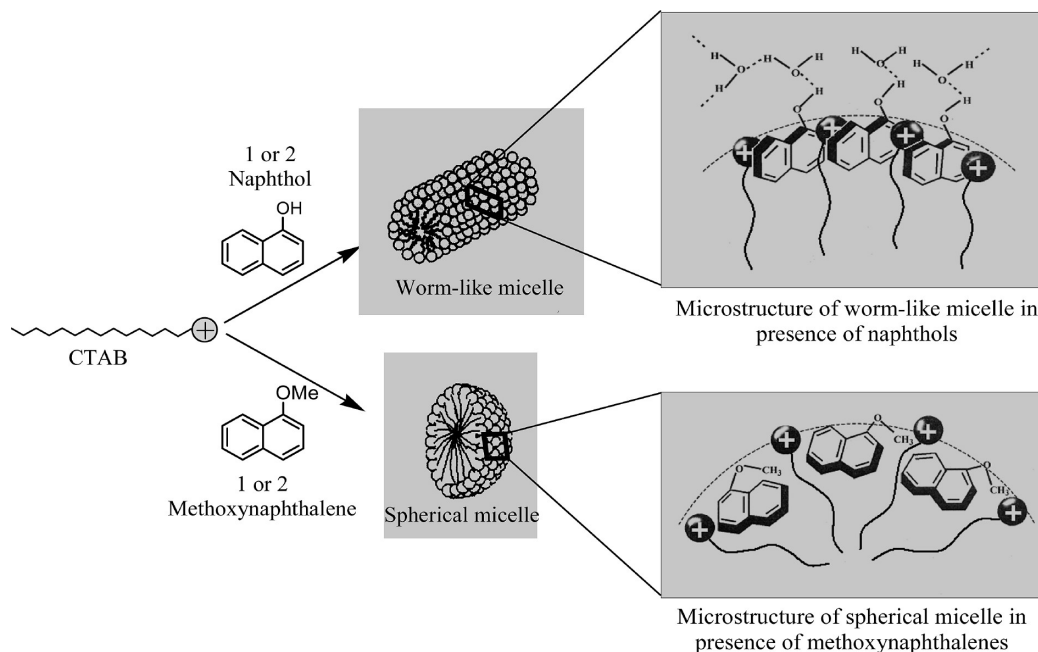


Figure 6. Schematic representation of the microstructures found in worm-like micelles formed by naphthols and spherical micelles formed by methoxynaphthalenes with CTAB.

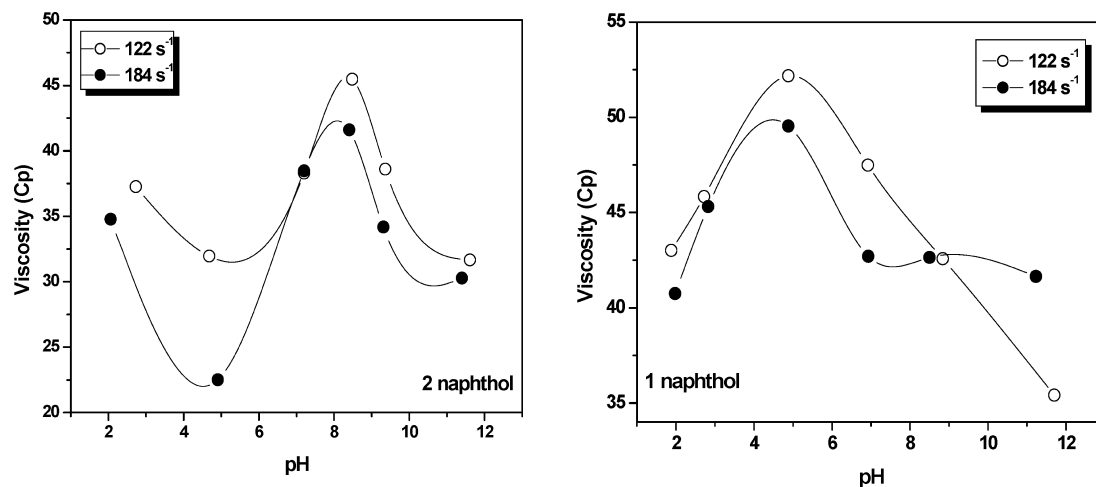


Figure 7. Viscosity vs pH profile for naphthol/CTAB systems at fixed shear rates of 122 and 184 s⁻¹.

that in naphthols indicates a weaker noncovalent interaction takes place. The large drop in intensity on first addition of 0.33 mM CTAB is the signature of breaking of a H-bond with bulk water molecules. Due to their directionality and spatial arrangement, complementary multiple H-bonding interactions at the micellar interface lead to engineering well-defined supramolecular structure via micellar headgroup charge shielding by π -electron systems of naphthols (Figure 6). This result of unusual H-bonding may be relevant, not only when considering the H-bonding of the interfacial water molecules in the specific micelle and dopant studied here but also for the H-bonding interaction of other micelle–dopant systems as well.

Shear-Induced Viscosity and pH. The role of neutral hydroxyaromatic dopants, viz., 1- and 2-HN, which are found to be efficient in bringing about microstructural transition in CTAB and CPB micelles, stimulates the idea of designing a route for pH-responsive vesicle formation.⁵ This idea stems from the fact that the dopants, which under neutral conditions activate the formation of worm-like micelles at pH \sim 5.0, may on partial ionization of the OH group increase the packing parameter further via charge screening. This idea tempted us to study the

pH dependent viscosity changes of the present viscoelastic gel system.³⁸ Figure 7 shows the viscosity–pH profiles of the 1-HN–CTAB and 2-HN–CTAB systems at constant shear of 122 and 184 s⁻¹, respectively. The general nature of the variation of viscosity as a function of pH for both 1- and 2-naphthol–CTAB systems is similar in high shear regime (viz., 122 and 184 s⁻¹, respectively). However, morphological responses are not identical for both of the systems. While the viscosity of both, 2- as well as 1-HN–CTAB systems, is quite high (35–45 Cp) due to formation of long worm-like micelles at low pH, the viscosity of the former system falls initially, indicating formation of shorter micelles with pH until pH \sim 5.0 is reached. On the other hand, for 1-HN–CTAB, the onset of viscosity rise as a function of pH is found to occur from very low pH (pH \sim 2.0). For 2-naphthol–CTAB, the onset of viscosity rise is observed at higher pH ($>$ 5.0) and the viscosity–pH profile passes through a maximum at pH \sim 8.5. The onset of viscosity rise is observed due to the partial titration of OH group, leading to charge screening of surfactant head groups by the naphtholate anion and at pH \sim 8.5 the worm-like micelles grow maximum. Further increase in pH results in the ionization of OH group further,

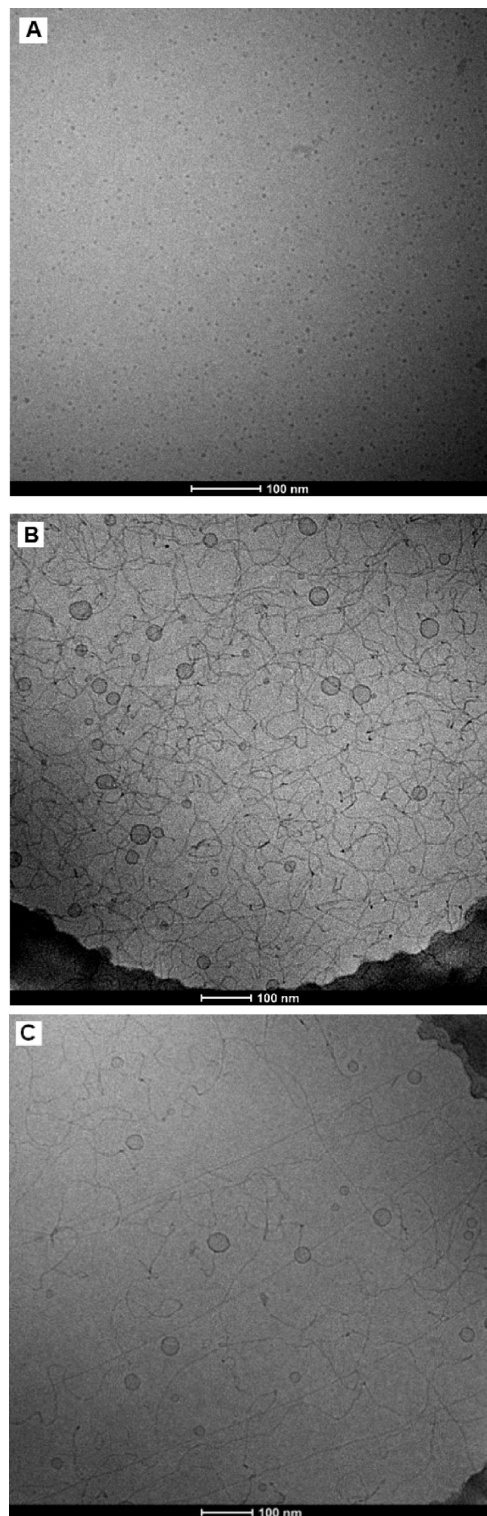


Figure 8. cryo-TEM micrographs of the CTAB–2-naphthol system (10 mM, 1:1) at normal pH (~ 5.5) (A) and at high pH (~ 9.4) (B). Part C shows linearly elongated worm-like micelles under shear flow.

and the packing parameter probably exceeds the critical value of $1/2$ via enhanced charge screening, leading to vesicle formation (for naphthols, $pK_a > 9$, which means 50% ionization of the OH group at pH ~ 9.0). This results in the fall of viscosity of the system. Since 1-naphthol could modulate the micellar surface curvature more efficiently, a little dissociation of the OH group (at low pH range) leads to an appreciable decrease of surface curvature via charge screening and promotes long

worm-like micelle formation. In fact, for the 1-HN–CTAB system, vesicles start to form even at slightly higher than pH ~ 5.0 (Figure 7). A simple and effective route to design pH-responsive viscoelastic worm-like micelles and less viscous globular vesicles based on naphthol dopants may be tuned by controlling the degree of charge screening of CTAB micelles via controlled ionization of naphtholic OH groups. The result of pH-responsive morphology modification is further investigated by means of cryo-TEM.

Cryogenic Transmission Electron Microscopic Study.

Cryo-TEM images of the CTAB–2-naphthol system at low and high pH's are shown in Figure 8. At low pH (pH ~ 5.5), the micrograph looks like a condense, isotropic, and continuous network (Figure 8A) of worm-like micelles along with mono-dispersed vesicles of very short diameters.

The micelles are slightly entangled. At high pH (pH ~ 9.4), the system contains very long (endless in micrograph) worm-like micelles, which coexist with large unilamellar vesicles. This is undoubtedly due to enhanced charge screening of micelles by naphtholate anions. The field is seen to populate mainly by large vesicles of diameter ~ 30 nm along with thinly populated smaller vesicles. It is also seen that the long worm-like micelles are highly entangled. Sometimes they are found to elongate linearly under shear flow (Figure 8c). The solutions are completely transparent. The direct imaging by cryo-TEM supports the rheological observation as a function of pH (Figure 7). At low pH, the worm-like micelles are formed via headgroup charge shielding by aromatic π electrons, whereas, at high pH, ionization of OH groups takes place and the packing parameter exceeds the critical value of $1/2$ via enhanced charge screening by naphtholate ion. This leads to unilamellar vesicle formation along with long worm-like micelles.

Conclusion

Neutral naphthols and methoxynaphthalenes, both with an aromatic π -system in their structures, are fairly surface active and embedded in aqueous CTAB micelles strongly. However, unlike methoxynaphthalenes, only naphthols can promote spherical to long worm-like micellar transition at room temperature and impart strong viscoelasticity and unusual rheology to the system. The success of naphthols in effecting micro-structural transition of micelles lies in their unique ability to form H-bonds with interfacial water molecules, which have shown unusual H-bond donating properties compared to bulk water. The OH groups of micelle-embedded naphthols are protruded toward the Stern layer through ~ 1 Å and the dielectric constant of OH sites has been measured as 45 ± 2 by observing the pK_a shift of acid–base equilibrium of naphthols at the interface relative to that in bulk water. The result of unusual H-bonding may be relevant, not only when considering the H-bonding of the interfacial water molecules in the specific micelle and dopant studied here but also for the H-bonding interaction of other micelle–dopant systems as well. On the basis of hydroxyaromatic dopants like naphthols, a simple and effective route to design pH-responsive viscoelastic worm-like micelles and the vesicles of single tail cationic surfactant (CTAB) is reported. Results are confirmed by observing cryogenic transmission electron microscopy (cryo-TEM) images.

Acknowledgment. The authors are thankful to Council of Scientific and Industrial Research, New Delhi, for financial support. Dr. Wins Busing of FEI Company, The Netherlands, is gratefully acknowledged for help in acquiring the cryo-TEM data.

References and Notes

- (1) Hoeben, F. J. N.; Jonkheijm, P.; Meijer, E. W.; Schenning, A. P. J. H. *Chem. Rev.* **2005**, *105*, 1491–1498.
- (2) Guldi, D. M.; Zerbetto, F.; Georgakilas, V.; Prato, M. *Acc. Chem. Res.* **2005**, *38*, 38–42.
- (3) Yoosaf, K.; Belbakra, A.; Nichola, A.; Llanes-Pallas, A. *Chem. Commun.* **2009**, 2830–2832.
- (4) Cui, S.; Liu, H.; Gan, L.; Li, Y.; Zhu, D. *Adv. Mater.* **2008**, *20*, 2918–2923.
- (5) Saha, S. K.; Jha, M.; Ali, M.; Chakraborty, A.; Bit, G.; Das, S. K. *J. Phys. Chem. B* **2008**, *112*, 4642–4647.
- (6) Tan, G.; Ford, C.; John, V. T.; He, J.; McPherson, G. L.; Bose, A. *Langmuir* **2008**, *24*, 1031–1036.
- (7) Isayama, M.; Nomiyama, K.; Yamaguchi, T.; Kimizuka, N. *Chem. Lett.* **2005**, *34*, 462–463.
- (8) Singh, M.; Ford, C.; Agarwal, V.; Fritz, G.; Bose, A.; John, V. T.; McPherson, G. L. *Langmuir* **2004**, *20*, 9931–9937.
- (9) Clint, J. H. *Surfactant Aggregation*; Blakie & Son Ltd.: London, 1992; p 147.
- (10) Manohar, C. In *Micelles, Microemulsions and Monolayers, Science and Technology*; Shah, O. D., Ed.; Marcel Dekker, Inc.: New York, 1998; p 145.
- (11) Davis, T. S.; Ketner, A. M.; Raghavan, S. R. *J. Am. Chem. Soc.* **2006**, *128*, 6669–6675.
- (12) Tung, S.-H.; Lee, H.-Y.; Raghavan, S. R. *J. Am. Chem. Soc.* **2008**, *130*, 8813–8817.
- (13) Israelachvili, J. N.; Mitchell, D. J.; Ninham, B. N. *J. Chem. Soc., Faraday Trans. 2* **1976**, *72*, 1525–1568.
- (14) Rehage, H.; Hoffman, H. *J. Phys. Chem.* **1988**, *92*, 4712–4719.
- (15) Rehage, H.; Hoffman, H. *Mol. Phys.* **1991**, *74*, 933–943.
- (16) Cates, M.; Candau, S. J. *J. Phys.: Condens. Matter* **1990**, *2*, 6869–6877.
- (17) Hu, Y.; Rajaram, C. V.; Wang, S. Q.; Jamieson, A. M. *Langmuir* **1994**, *10*, 80–85.
- (18) Ketner, A. M.; Kumar, R.; Davies, T. S.; Elder, P. W.; Raghavan, S. R. *J. Am. Chem. Soc.* **2007**, *129*, 1553–1557.
- (19) Keller, S. L.; Boltenhagen, P.; Pine, D. J.; Zasadzinski, J. A. *Phys. Rev. Lett.* **1998**, *80*, 2725–2728.
- (20) Boltenhagen, B.; Hu, Y.; Matthys, E. F.; Pine, D. J. *Phys. Rev. Lett.* **1997**, *79*, 2359–2362.
- (21) Liu, C.; Pine, D. J. *Phys. Rev. Lett.* **1996**, *77*, 2121–2124.
- (22) Zheng, Y.; Lin, Z.; Zakin, J. L.; Talmon, Y.; Davis, H. T.; Scriven, L. E. *J. Phys. Chem. B* **2000**, *104*, 5263–5271.
- (23) Mendes, E.; Narayanan, J.; Oda, R.; Kern, F.; Candau, S. J. *J. Phys. Chem. B* **1997**, *101*, 2256–2258.
- (24) Agarwal, V.; Singh, M.; McPherson, G.; John, V.; Bose, A. *Colloids Surf., A* **2006**, *281*, 246–253.
- (25) Dougherty, D. A. *Science* **1996**, *271*, 163–168.
- (26) Drummond, C. J.; Grieser, F.; Healy, T. W. *J. Chem. Soc., Faraday Trans. 1* **1989**, *85*, 521–535.
- (27) Drummond, C. J.; Grieser, F.; Healy, T. W. *J. Chem. Soc., Faraday Trans. 1* **1989**, *85*, 537–550.
- (28) Mishra, B. K.; Samant, S. D.; Pradhan, P.; Mishra, S. B.; Manohar, C. *Langmuir* **1993**, *9*, 894–898.
- (29) Drummond, C. J.; Grieser, F.; Healy, T. W. *Faraday Discuss. Chem. Soc.* **1986**, *81*, 95–102.
- (30) Lamm, G.; Pack, G. R. *J. Phys. Chem. B* **1997**, *101*, 959–965.
- (31) Baba, H.; Suzuki, S. *J. Chem. Phys.* **1961**, *35*, 1118–1127.
- (32) Nemethy, G.; Ray, A. *J. Phys. Chem.* **1973**, *77*, 64–68.
- (33) Zharkova, O. M.; Korolev, B. V.; Morozova, Y. P. *Russ. Phys. J.* **2003**, *46*, 68–74.
- (34) Ramachandran, C.; Pyter, R. A.; Mukherjee, P. *J. Phys. Chem.* **1982**, *86*, 3198–3205.
- (35) Bhattacharya, K. *J. Fluoresc.* **2001**, *11*, 167–179.
- (36) Balasubramanian, S.; Pal, S.; Bagchi, B. *Curr. Sci.* **2002**, *82*, 845–848.
- (37) Gasjo, J.; Anderson, E.; Forsberg, J.; Aziz, E. F.; Brena, B.; Johansson, C.; Nordgren, J.; Duda, L.; Adersson, J.; Hennies, F.; Rubensson, J.; Hansson, P. *J. Phys. Chem. B* **2009**, *113*, 8201–8205.
- (38) Lin, Y.; Han, X.; Huang, J.; Fu, H.; Yu, C. *J. Colloid Interface Sci.* **2009**, *330*, 449–455.

JP907677X